ELSEVIER

Journal of Molecular Catalysis A: Chemical 144 (1999) 137–150

JOURNAL OF MOLECULAR CATALYSIS A: CHEMICAL

www.elsevier.com/locate/molcata

# Borane-functionalized oxide supports: development of active supported metallocene catalysts at low aluminoxane loading

Jun Tian, Shaotian Wang, Yuding Feng, Jieming Li, Scott Collins *

*Department of Chemistry, University of Waterloo, Waterloo, Ontario, Canada N2L 3G1*

Received 17 July 1998; accepted 30 September 1998

**Abstract**

Treatment of hydroxylated silica or alumina with tris(perfluorophenyl)borane (**1**), bis(perfluorophenyl)borane (**2**) or bis(perfluorophenyl)boron chloride (**3**), provides borane-functionalized supports of variable composition, as revealed by in situ monitoring by $^{19}F$ NMR spectroscopy and/or elemental analysis. These chemically treated supports can be impregnated with $Cp_2ZrMe_2$ to provide supported catalysts for ethylene polymerization. Although some of these supported catalysts are active for ethylene polymerization in the presence of alkylaluminum compounds (e.g., TMA, TIBAL), all of these catalysts are more efficiently activated in the presence of small quantities of methyl aluminoxane, even at very low Al:Zr ratios of 10:1. The polymer properties are quite similar to those produced using the soluble catalyst $Cp_2ZrMe_2/B(C_6F_5)_3$, again in the presence of MAO at low loading. A variety of experiments suggest that minimal leaching of the metallocene complex from the support occurs under the conditions studied; in particular, production of polyethylene with high bulk densities ($> 0.2$ g/cm$^3$) and little reactor fouling, even at elevated temperature in toluene slurry, is observed. 

*Keywords:* Boron; Supported-metallocene; Olefin polymerization

## 1. Introduction

The development of effective, supported metallocene catalysts for olefin polymerization continues to attract attention [1–3]. The most common approach involved impregnation of hydroxylated silica with methyl aluminoxane (MAO), followed by treatment with a metallocene complex [4–16]. These materials are active for olefin polymerization, particularly in the context of gas-phase polymerization processes [15,16], or in slurry polymerizations in the presence of additional MAO [4–10,14,16] or other alkylaluminum compounds [11–13]. More recently, alternative approaches have been described, where silica is functionalized with a single component co-catalyst (e.g., $[SiO_2–OB(C_6F_5)_3][Ph_3C]$) and this chemically modified support is used in combination with a metallocene dialkyl complex in

* Corresponding author

1381-1169/99/$ - see front matter 
PII: S1381-1169(98)00341-0

olefin polymerization [17–21]. Although such supported catalysts are active for ethylene polymerization in the absence of MAO, they are less active than those based on MAO-treated silica.

It had occurred to us that a complementary approach might involve functionalization of hydroxylated silica or alumina with organoboranes. By analogy to the work of Siedle and coworkers [22,23], use of $B(C_6F_5)_3$ (**1**) might lead to surface-bound, silanol-borane adducts which might activate dialkylzirconocene complexes for ethylene polymerization (Eq. (1)).

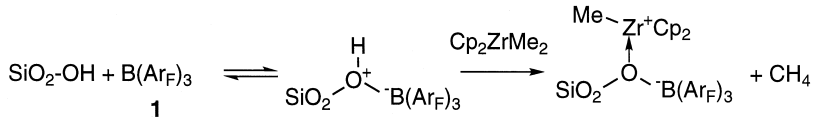


(1)

Alternatively, use of reactive organoboranes such as $HB(C_6F_5)_2$ (**2**) [24] or $ClB(C_6F_5)_2$ (**3**) [25] might provide surface-bound, borinic esters (Eq. (2)), that might be sufficiently Lewis acidic to also activate dialkylmetallocene complexes.

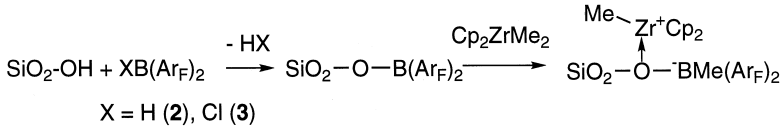


(2)

Based on the work of Feher and coworkers [26–29] and Hermann et al. [30] using model sesquisiloxanes, the electron-withdrawing power of a tri-functional surface site on silica (e.g., as in **4**) is similar to that of a $CF_3$ group and this should render the surface-bound organoborane much more Lewis acidic.

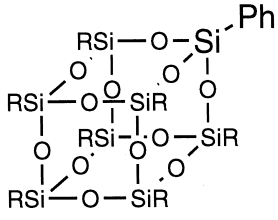


**4**: R = $^{c}$Hx

Herein, we report the results of both synthetic studies and olefin polymerization experiments that reveal that this approach can be effective, particularly in the presence of dramatically reduced quantities of MAO.

## 2. Functionalization of silica and alumina with organoboranes

Partially dehydroxylated silica was prepared by calcination of fully hydroxylated material, while fully hydroxylated alumina was prepared from dehydroxylated alumina as previously described [16]. The surface hydroxyl group concentration was determined by titration with $AlMe_3$ and the properties of the supports employed are summarized in Table 1.

Table 1
Properties of supports used

| Support | Code | Surface area ($m^2/g$) | Pore volume (ml/g) | Pore radius (Å) | OH content (mmol OH/g) |
|---|---|---|---|---|---|
| PQ $SiO_2$ | PQ | 440 | 3.1 | 144 | 1.30 |
| Ketjen $Al_2O_3$ | KG | 326 | 0.73 | 45 | 3.02 |

These hydroxylated supports were then treated with an equivalent of organoboranes **1**–**3** (based on surface OH content) in toluene slurry to provide borane functionalized supports. Following filtration, washing and drying, chemically modified silicas and aluminas were produced and based on fluorine analyses of some of these materials, [1] significant organoborane was incorporated (Table 2).

These reactions were also indirectly monitored by $^{19}F$ NMR in toluene-$d_8$ suspension in the presence of an internal standard to determine the extent of incorporation of the borane as well as the production of any soluble by-products arising from chemical reaction with the support. The amount of borane incorporated on the support, as measured by this technique (Table 2), was found to be much higher than that based on chemical analysis for reactions involving borane **1**; we suspect this arises from reversible binding of borane **1** to hydroxylated silica or alumina (Eq. (1)), so that during washing of the support, significant loss of borane occurs, compared to the 'equilibrium' value as measured by NMR.

Quite high levels of compounds **2** and **3** could be deposited on silica (ca. 70–80% yield with respect to surface OH content, Table 2), whereas only small amounts (on a per mole basis) of organoborane **1** were adsorbed on this support (ca. 7 wt.%). There was little, if any, by-product formation observed in all three cases as judged by the absence of $C_6F_5H$, $HOB(C_6F_5)_2$ or the corresponding anhydride $O[B(C_6F_5)_2]_2$ (hydrolysis products of **1**–**3**). [2]

Interestingly, quite different behavior was observed using alumina; here, **1** was adsorbed in the largest quantities (again without decomposition, as judged by the absence of any soluble by-products) whereas compound **3** appears to dehydrate the alumina as judged by the quantitative and clean formation of $O[B(C_6F_5)_2]_2$ (formed from reaction of **3** with $HOB(C_6F_5)_2$ in solution). [2,3]

## 3. Adsorption of dimethylzirconocene on borane-functionalized supports

The chemically modified supports PQ-**1** to PQ-**3**, and KG-**1** were contacted with an excess (based on surface OH content of the untreated supports) of $Cp_2ZrMe_2$ in toluene suspension to provide supported catalysts, following filtration, washing and drying. Again, in addition to Zr analysis on the final materials, the reaction of excess $Cp_2ZrMe_2$ with these supports was indirectly monitored by $^1H$ NMR in benzene-$d_6$ suspension to determine the extent of reaction and the formation of any soluble by-products. In all cases, less $Cp_2ZrMe_2$ was adsorbed, based on final Zr-content, as determined by analysis, than was predicted based on the NMR experiments (Table 3); we suspect this discrepancy

[1] Reproducible analyses for B in the presence of Al or Si proved problematic.

[2] Independent synthesis of $(C_6F_5)_2BOH$ can be performed through either hydrolysis of **2** and **3** at room temperature, or hydrolysis of **1** at elevated temperatures; the corresponding anhydride is available by reaction of $(C_6F_5)_2BOH$ with **3** at room temperature in toluene solution (see Section 8). We thank Prof. Warren Piers (U. Calgary) for providing spectroscopic data for authentic samples of $HOB(C_6F_5)_2$.

[3] Compound **2** appeared to show very complicated behavior with alumina (i.e., appearance of multiple by-products not corresponding solely to hydrolysis) and the resulting support was not further investigated.

Table 2
Adsorption of boranes on supports

| Support | Borane | Wt.%[a] | Wt.%[b] | Surface B:OH[c] | Code |
|---|---|---|---|---|---|
| PQ | **1** | 6.80 | 18.2 | 0.10 | PQ-**1** |
| PQ | **2** | 26.3 | 25.7 | 0.80 | PQ-**2** |
| PQ | **3** | 24.2 | 25.4 | 0.71 | PQ-**3** |
| KG | **1** | 20.6 | 47.3 | 0.17 | KG-**1** |
| KG | **3** | trace | 0.0 | 0.0 | KG-**3** |

[a] Wt.% $BR_3$ or $BR_2$ incorporated as determined by neutron activation analysis.
[b] Wt.% $BR_3$ or $BR_2$ incorporated as determined indirectly by NMR.
[c] Calculated value based on neutron activation analysis.

Table 3
Adsorption of $Cp_2ZrMe_2$ on borane-treated supports

| Support | Wt.% Zr[a] | Wt.% Zr[b] | Wt.% B[c] | Zr:B[d] | Code |
|---|---|---|---|---|---|
| PQ-**1** | 4.41 | – | 6.80 | 3.57 | PQ-**1**-Zr |
| PQ-**2** | 4.68 | 4.98 | 19.4 | 0.91 | PQ-**2**-Zr |
| PQ-**3** | 3.63 | 4.66 | 13.9 | 0.96 | PQ-**3**-Zr |
| KG-**1** | 3.81 | 4.04 | 13.3 | 1.16 | KG-**1**-Zr |
| PQ | 6.42[e] | 8.25 | – | – | PQ-Zr |
| KG | 6.74[e] | 8.86 | – | – | KG-Zr |

[a] Wt.% Zr present as determined by neutron activation analysis.
[b] Wt.% Zr incorporated as determined indirectly by NMR.
[c] Wt.% $BR_3$ or $BR_2$ calculated based on *F*-analysis.
[d] Calculated values based on neutron activation analysis.
[e] Wt.% Zr present as determined by weight difference.

arises, in some cases, because of reversible binding and/or decomposition during isolation and washing.

Monitoring of these reactions by NMR proved informative as, in certain cases, soluble byproducts were detected. For reactions involving either PQ-**1** or KG-**1** (or PQ and KG), the only by-product detected was methane. [4] Qualitatively, less was evolved in the reactions involving the chemically treated supports compared with their hydroxylated counterparts. As might be expected, larger quantities of $Cp_2ZrMe_2$ can be deposited on untreated PQ silica and alumina. In these cases, it is known that the surface-bound species are principally $SiO_2$–$OZr(Me)Cp_2$ and $Al_2O_3$–$OZr(Me)Cp_2$ [31,32].

In the case of PQ-**1** it is clear that the dominant process occurring involves reaction of $Cp_2ZrMe_2$ with surface-OH groups as considerably more Zr was deposited onto this support than would be predicted if the reaction proceeded according to Eq. (1) (i.e., the surface Zr:B ratio was much greater than 1, Table 3); in contrast, KG-**1** reacted with $Cp_2ZrMe_2$ in a manner consistent with the stoichiometry indicated in Eq. (1) as the final Zr:B ratio was close to 1.

In the case of both PQ-**2** and PQ-**3** significant amounts of by-products were detected in solution. These were identified as $Me_2B(Ar_F)$ and $Cp_2ZrMe(Ar_F)$ and were formed in the amounts indicated in Eq. (3). These products also form from $MeB(Ar_F)_2$ and $Cp_2ZrMe_2$ in toluene solution at room

[4] Interestingly, the compound $Cp_2ZrMe(\mu\text{-}Me)B(C_6F_5)_3$ was not detected in solution; this would be expected product from reaction of $Cp_2ZrMe_2$ with $B(C_6F_5)_3$ (using PQ-**1** or KG-**1**).

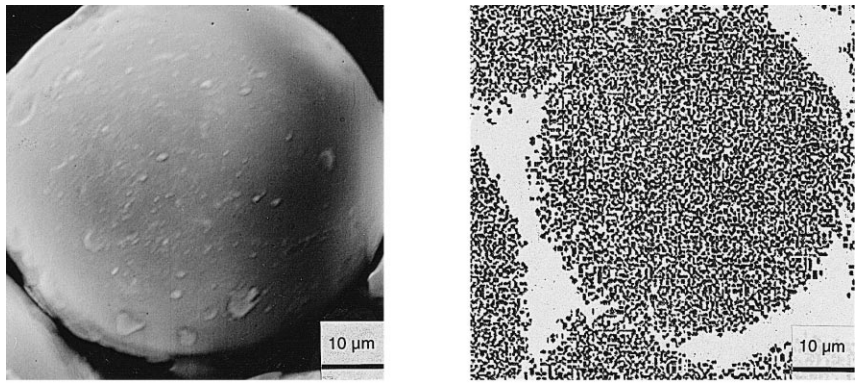


Fig. 1. (a) SEM micrograph of PQ-**3**-Zr catalyst particle and (b) zirconium distribution as measured by energy-dispersed, X-ray microanalysis.

temperatures, via the ion pair $[Cp_2ZrMe][Me_2B(Ar_F)_2]$, a species, which was also detected at low conversion in a separate experiment (see Section 8). [5] Thus, the formation of $Me_2B(Ar_F)$ and $Cp_2ZrMe(Ar_F)$ suggests that $MeB(Ar_F)_2$ is produced on reaction of $Cp_2ZrMe_2$ with these supports and a plausible mechanism for this is depicted in Eq. (4).

$$\mathrm{SiO_2{-}O{-}B(Ar_F)_2} \xrightarrow[\text{(xs)}]{\mathrm{Cp_2ZrMe_2}} \mathrm{Cp_2ZrMe(Ar_F) + Me_2BAr_F} \quad \text{(via } [Cp_2ZrMe][Me_2B(Ar_F)_2]\text{)} \tag{3}$$

PQ-**2** 22 % of total $Cp_2ZrMe_2$ consumed
PQ-**3** 34 % of total $Cp_2ZrMe_2$ consumed

$$\mathrm{SiO_2{-}O{-}B(Ar_F)_2} \xrightarrow{\mathrm{Cp_2ZrMe_2}} \mathrm{SiO_2{-}O{-}\overset{\mathrm{Me}}{\underset{}{B}}(Ar_F)_2\,Zr^{+}Cp_2} \xrightarrow{-\,\mathrm{MeB(Ar_F)_2}} \mathrm{SiO_2{-}O{-}ZrMeCp_2} \tag{4}$$

In agreement with this hypothesis, the fluorine content (i.e., $BR_2$ content) of both PQ-**2**-Zr and PQ-**3**-Zr was considerably lower (Table 3) than would be predicted if the only reaction occurring was ion-pair formation on the surface (Eq. (2)). In fact, when the formation of $MeB(Ar_F)_2$ is taken into account, the surface stoichiometry of Zr:B is close to 1:1 in the final supported catalysts (Table 3).

Of the various supports prepared, PQ-**2**-Zr, PQ-**3**-Zr and KG-**1**-Zr were obtained as yellow-orange powders whereas PQ-**1**-Zr, PQ-Zr, and KG-Zr were formed as off-white solids. This suggests that only in the former three cases, were cationic complexes formed on the support; clearly the origins of the differences seen, both during reaction of these supports with boranes, and also with $Cp_2ZrMe_2$ are of some fundamental interest.

## 4. Zirconium distribution on the supported catalysts

The spatial distribution of zirconium on the porous silica particles is illustrated by SEM micrographs of the supported catalyst PQ-**3**-Zr, where the particle size was ca. 50 μm (Fig. 1). Upon

[5] For related observations using $Cp''_2ZrMe_2$ [$Cp'' = 1,3\text{-}(Me_3Si)_2Cp$] and $MeB(Ar_F)_2$, see Ref. [33].

focusing on the same observation region, the macroscopic distribution of zirconium was detected by means of an energy-dispersed X-ray microanalyzer (EDX); as shown in Fig. 1b, the black patches, which represent Zr-rich sites, are dispersed uniformly on the support.

## 5. Ethylene polymerization with supported catalysts

Ethylene polymerizations using the catalysts prepared were conducted in toluene slurry using TIBAL as a scrubbing agent (Al:Zr = 10:1) under a variety of conditions, and the results are summarized in Table 4. Of the various materials prepared, only PQ-**2**-Zr, PQ-**3**-Zr and KG-**1**-Zr exhibited any activity for ethylene polymerization in the absence of MAO (Table 4 entries 1, 2 and 14); having said that the productivities based on both Zr or the amount of support employed, leave much to be desired. These experiments suggest that very little, 'active' cationic zirconocene complex is present on these three supports. However, as indicated in Table 4, pre-contacting PQ-**1**-Zr, PQ-**2**-Zr, PQ-**3**-Zr, and KG-**1**-Zr with small quantities of MAO in toluene (typically at 50:1 Al:Zr levels), led to dramatic improvements in catalytic activity (Table 4, entries 3–7, 15). Of these supports, PQ-**1**-Zr is the most active (based on Zr) or on the amount of supported catalyst (entry 3) while the productivities of PQ-**3**-Zr and KG-**1**-Zr are comparable (entries 5 and 15) and PQ-**2**-Zr is the least active (entry 4). The activity of all of these catalysts is superior/comparable to a

Table 4
Ethylene polymerization with supported catalysts[a]

| Entry | Catalyst | Al:Zr[b] | $T$ (°C) | $A_1^c$ | $A_2^d$ |
|---|---|---|---|---|---|
| 1 | PQ-**2**-Zr | 0 | 30 | 31[e] | 0.016 |
| 2 | PQ-**3**-Zr | 0 | 30 | 37[e] | 0.014 |
| 3 | PQ-**1**-Zr | 50 | 70 | 10.6 | 5.07 |
| 4 | PQ-**2**-Zr | 50 | 70 | 4.75 | 2.45 |
| 5 | PQ-**3**-Zr | 50 | 70 | 9.33 | 3.72 |
| 6 | PQ-**3**-Zr | 25 | 30 | 1.26 | 0.50 |
| 7 | PQ-**3**-Zr | 10 | 30 | 0.329 | 0.13 |
| 8 | PQ-Zr | 50 | 70 | 7.48 | 5.88 |
| 9 | PQ-Zr | 25 | 70 | 3.63 | 2.85 |
| 10 | PQ-Zr | 10 | 70 | 3.58 | 2.82 |
| 11 | PQ-MAO-Zr | 50 | 70 | 4.88 | 1.35 |
| 12 | PQ-**3**-Zr[f] | 50 | 70 | – | 0.033 |
| 13 | PQ-Zr[f] | 50 | 70 | – | 0.023 |
| 14 | KG-**1**-Zr | 0 | 30 | 42[e] | 0.006 |
| 15 | KG-**1**-Zr | 50 | 70 | 10.2 | 3.57 |
| 16 | KG-Zr | 50 | 70 | 2.10 | 1.67 |
| 17 | KG-MAO-Zr | 50 | 70 | 7.89 | 2.10 |
| 18 | KG-MAO-Zr | ca. 20[g] | 70 | 1.01 | 0.267 |
| 19 | KG-**1**-Zr[f] | 50 | 70 | – | 0.010 |
| 20 | $Cp_2ZrMe_2$ | 50 | 70 | 0.92 | – |
| 21 | $Cp_2ZrMe_2$[h] | 50 | 70 | 4.52 | – |

[a] Conditions: toluene (500 ml), TIBAL (10:1 Al:Zr), $C_2H_4$ (75 psig), 1000 rpm.
[b] Total Al:Zr ratio (as MAO).
[c] Activity in $10^3$ kg PE/mol Zr×h.
[d] Activity in kg PE/g support×h.
[e] Activity in kg PE/mol Zr×h.
[f] Polymerization with toluene soluble portion, following filtration.
[g] Surface Al:Zr ratio—see Ref. [16].
[h] $Cp_2ZrMe_2$ treated with a slight excess (1.1 equiv. of $B(C_6F_5)_3$.

Table 5
Properties of PE prepared with supported catalysts

| Entry | Catalyst | Conditions[a] | $M_w$ ($10^5$) | $M_w / M_n$ | $T_m$ (°C)[b] | Bulk density[c] ($g/cm^3$) |
|---|---|---|---|---|---|---|
| 1 | PQ-**1**-Zr | 3 | 1.97 | 2.04 | 129.8 | 0.43 |
| 2 | PQ-**2**-Zr | 4 | 2.11 | 2.10 | 127.7 | 0.39 |
| 3 | PQ-**3**-Zr | 5 | 1.89 | 2.10 | 129.0 | 0.41 |
| 4 | PQ-Zr | 8 | 1.71 | 2.53 | 134.9 | 0.49 |
| 5 | KG-**1**-Zr | 15 | 1.89 | 1.90 | 126.2 | 0.32 |
| 6 | $Cp_2ZrMe_2$ | 20 | 2.57 | 2.16 | 129.0 | 0.17 |
| 7 | $Cp_2ZrMe_2$ | 21 | 2.88 | 2.89 | 122.8 | 0.16 |

[a] The number refers to the corresponding entry in Table 4.
[b] Peak melting temperature as measured by DSC.
[c] Bulk density measured according to Ref. [35].

conventional supported catalyst based on MAO-impregnated silica or alumina (entries 11 and 17) at similar (total) loadings of MAO.

Quite surprisingly, PQ-Zr proved to be an active catalyst in the presence of reduced quantities of MAO. This finding suggests that MAO is capable of cleaving Si–O–Zr bonds to provide active catalyst (perhaps via formation of $Cp_2ZrMe_2$ and $SiO_2$–OMAO, followed by ionization). [6] A comparison of this catalyst with, e.g., PQ-**3**-Zr (Table 4, entries 5–7 and 8–10), reveals that pre-treatment of silica with borane **3** appears to confer little, if any, advantage compared to direct reaction of silica with $Cp_2ZrMe_2$. In fact, at lower Al:Zr ratios, the performance of PQ-Zr is superior.

Somewhat different results were observed with the alumina-based catalysts. Of these KG-**1**-Zr is the most active formulation, being marginally superior to a conventional MAO-treated alumina (Table 4, entries 15 and 17) and considerably more active than alumina that is directly treated with $Cp_2ZrMe_2$ (entry 16).

While the productivities observed are much higher than that observed using $Cp_2ZrMe_2$/MAO under the same conditions (Table 4, entry 20), there is the obvious concern that significant leaching of soluble catalyst occurs during the pre-contacting period and/or during polymerization. [7] Although not exhaustively pursued for all combinations, control experiments that involved pre-contacting the support with MAO, filtration and use of the filtrate revealed that minimal leaching of metallocene complex was observed at this stage (Table 4, entries 12, 13, and 19). [8, 9]

## 6. Polymer properties

As is evident from the results summarized in Table 5, the nascent polyethylene produced by these supported catalysts has high bulk density ($> 0.3$ $g/cm^3$), and good particle morphology for

[6] We note that PQ-Zr appears to be unreactive towards a large excess of $AlMe_3$ (i.e., no $Cp_2ZrMe_2$ produced in toluene solution), suggesting that a component of MAO (other than $AlMe_3$) is responsible for this alkylation/ionization process.

[7] A recent report suggests that supported catalysts analogous to PQ-Zr undergo extensive leaching of metallocene complex; these results appear to be contrary to the findings reported here but may reflect the different treatments employed (i.e., large excess of MAO at elevated temperatures). See Ref. [34].

[8] Also, pre-polymerization with ethylene at an initial temperature of 25°C and 75 psig in a sample bomb, followed by filtration, washing and use of the filtrate in a subsequent polymerization (at 70°C/75 psig) also indicated minimal leaching (trace quantities of PE formed with either KG-**1**-Zr or PQ-Zr). We cannot, however, eliminate the possibility that leaching does occur under the conditions reported in Table 5 (70°C/75 psig). See Ref. [34].

[9] $^1H$ NMR experiments also showed that no $Cp_2ZrMe_2$ or $Cp_2Zr^+Me$ appeared in solution within 20 min at room temperature on treatment of PQ-Zr with excess MAO in toluene-$d_8$.

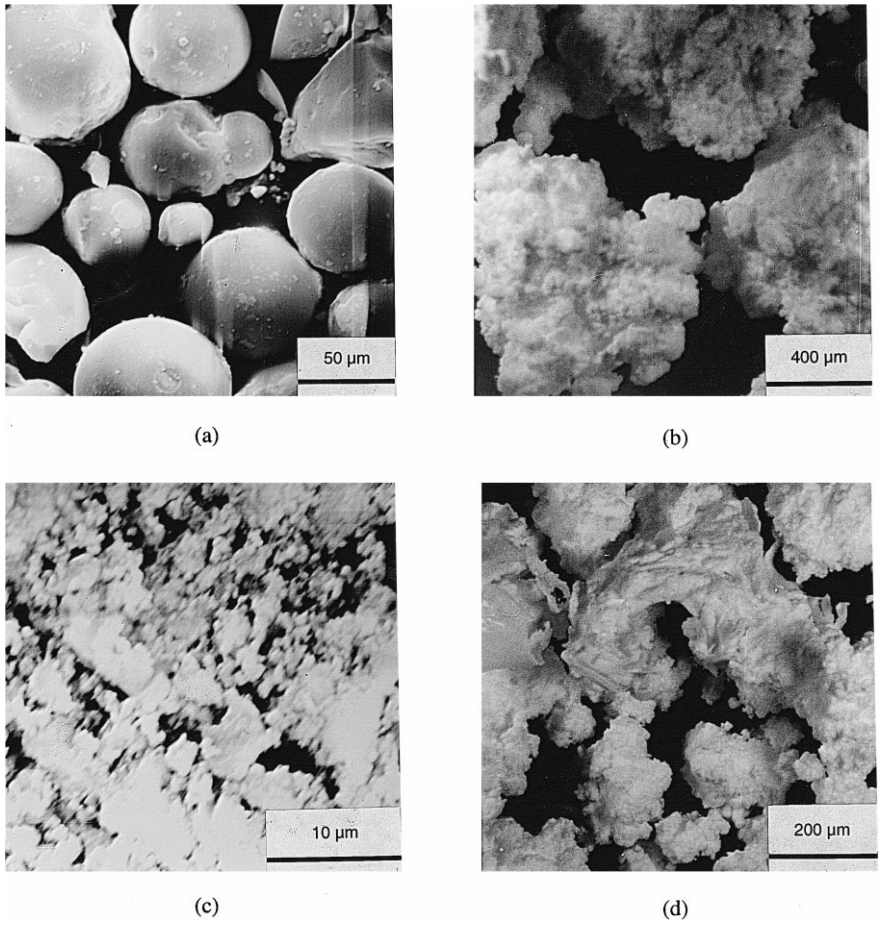


Fig. 2. SEM and optical microscope images of PQ-**3**-Zr and its nascent polyethylene [(a) and (b), respectively] and KG-**1**-Zr and its nascent polyethylene [(c) and (d), respectively].

silica-based catalysts (Fig. 2a and b), as shown by SEM and optical microscopy. However, the polymer product from the alumina-based catalyst (KG-**1**-Zr) had irregular shape and a broad size distribution, which more or less mirrored the properties of the alumina support itself (Fig. 2c and d). Also, minimal, if any, reactor fouling was observed, even at elevated temperatures in toluene slurry, conditions where leaching should be most problematic. Finally, as is evident from the MW data summarized in Table 5, comparable MWs and MWDs were observed with these supported catalysts as compared to use of a soluble catalyst under similar conditions.

## 7. Conclusions

As can be appreciated from this work, active formulations for supported catalysts can be derived from either silica or alumina by treatment with (a) either an organoborane, followed by treatment with a dialkylzirconocene or (b) direct treatment with dimethylzirconocene. Both approaches require pre-contacting with MAO for useful activity and paradoxically, this approach appears to be more efficient than first depositing MAO on the support in many cases. Having said that, there appears to

be no practical advantage in chemically pre-treating silica with an organoborane (except perhaps with borane **1**), while for alumina, the borane-treated support gives rise to a catalyst with marginally improved productivity. Quite clearly, further progress along these lines is hampered by the lack of knowledge concerning the Zr and B species that are present on the surface of these materials. Future work will focus on this important issue.

## 8. Experimental

All chemicals were reagent grade and purified as required prior to use. Diethyl ether, dichloromethane, tetrahydrofuran, hexane and toluene were dried and deoxygenated using a solvent purification system similar to that reported in the literature [36]. Benzene and pentane were dried and deoxygenated by distillation from sodium and benzophenone under nitrogen. Deuterated toluene and benzene for NMR spectroscopy were pre-dried and distilled in the same manner. All manipulations with air and moisture sensitive compounds were performed using standard Schlenk techniques under nitrogen. Air and moisture sensitive compounds were stored in either a Vacuum Atmosphere glove box or a Braun MB 150 M glove box. Methyllithium (Aldrich) was titrated immediately prior to use with 4-biphenylmethanol as described in the literature [37]. The compounds $Cp_2ZrMe_2$ [38], $HB(C_6F_5)_2$ (**2**) [24], and $ClB(C_6F_5)_2$ (**3**) [25] were synthesized according to literature procedures.

Routine $^1H$ NMR spectra were obtained on Bruker AM-250 or AC-200 spectrometer in the appropriate deuterated solvents; chemical shifts are referenced to residual undeuterated solvent. $^{19}F$ NMR spectra were recorded on Bruker AC-200 spectrometer and chemical shifts are referenced to 2,3,5,6-tetrafluoro-*p*-xylene, which was added as an internal standard and had already been referenced to $CFCl_3$ at the same recording conditions. $^{11}B$ NMR spectra were recorded on the same instrument and chemicals shifts were referenced to external standard $F_3B \cdot OEt_2$. The $^{11}B$ NMR spectra were obtained using a background substraction routine to remove resonances duo to borosilicate glass in the NMR probe and NMR tube. This was accomplished by recording the spectrum of an NMR tube containing the same height of pure solvent and with identical collection parameters to that of the sample and subtracting this background FID from that of the sample. Chemical shift data are summarized in Table 6. Neutron activation analyses were performed at the École Polytechnique, Montréal, PQ while conventional combustion analyses were performed by M.H.W. Laboratories of Phoenix, AZ.

Table 6
$^{19}F$ and $^{11}B$ NMR data for compounds prepared[a]

| Compound | $^{19}F$ (ppm) | | | $^{11}B$ (ppm) |
|---|---|---|---|---|
| | *o*-F | *p*-F | *m*-F | |
| **1** | −130.0 | −143.1[b] | −161.3 | 57.6 |
| **1**·$H_2O$ | −134.8 | −153.6 | −162.3 | 5.34 |
| **2** | −133.1 | −146.7 | −159.2 | 18.0[c] |
| **3** | −129.6 | −144.0 | −160.7 | 58.8 |
| $(C_6F_5)_2BOH$ | −133.1 | −148.3[b] | −161.4 | 40.2 |
| $[(C_6F_5)_2B]_2O$ | −132.6 | −144.3[b] | −160.2 | 40.1 |
| $C_6F_5H$ | −139.2 | −154.3 | −162.5 | – |

[a]All spectra were recorded in toluene-$d_8$ solution at 25°C at 188.0 and 64.2 MHz, for $^{19}F$ and $^{11}B$, respectively. For the acquisition of $^{11}B$ spectra, a blank sample was recorded in toluene-$d_8$ and then the same tube was used for sample preparation and the baseline was corrected by spectral subtraction.
[b]The chemical shift and/or line-width of this signal are sensitive to the presence of adventitious water in the sample and/or NMR solvents.
[c]Major component corresponding to dimer; minor component at 60.0 ppm corresponding to monomer (see Ref. [24]).

### 8.1. Support preparation

Silica available from Quantum Chemicals under the designation of PQ 3010, has a surface area of 440 $m^2/g$ and a pore volume of 3.10 $cm^3/g$ with an average pore radius 144 Å. Unless indicated otherwise, the silica used was washed with deionized water at room temperature, dried at 80°C under vacuum to constant weight, heated in a quartz tube inside a horizontal tube furnace to 500–600°C for 4 h under oxygen flow and then cooled down to room temperature under oxygen flow to produce partially dehydroxylated silica (PDS). The hydroxyl group content was determined by titration with trimethylaluminum, and the content was 1.30 mmol OH/g support.

Ketjen G alumina (Akzo Nobel) had a surface area of 326 $m^2/g$ and a pore volume of 0.73 $cm^3/g$ with an average pore radius 45 Å. It was washed with deionized water and then heated at 500°C for 3 h under oxygen flow, to form partially dehydroxylated alumina (PDA) with a hydroxyl content of 0.19 mmol/g support. PDA was then heated under water-saturated nitrogen for 48 h at 300°C to provide fully hydroxylated alumina (FHA). The hydroxyl group content was 3.02 mmol OH/g.

### 8.2. Preparation of PQ-*1*

To a mixture of 1.000 g silica (1.305 mmol OH) and 0.690 g $B(C_6F_5)_3$ (1.305 mmol) was added 20 ml toluene at room temperature. The slurry was stirred in the glove box for 18 h. A white solid was collected on a medium fritted funnel, washed with toluene ($4 \times 5$ ml) and dried in vacuo at room temperature. The weight was 1.056 g. Analytical data appear in Table 2.

### 8.3. Preparation of PQ-*2* and PQ-*3*

The same procedure as reported for PQ-**1** was followed, except that the reaction time was 3 h, with the following reagents: 1.000 g silica (1.305 mmol) in each case, and 0.451 g of **2** (1.305 mmol) and 0.496 g of **3** (1.305 mmol), for the preparation of PQ-**2** (1.384 g) and PQ-**3** (1.480 g), respectively. Analytical data appear in Table 2.

### 8.4. Preparation of KG-*1*

Twenty milliliters of toluene was added with vigorous stirring to a mixture of 0.788 g alumina (2.630 mmol OH) and 1.347 g of **1** (2.630 mmol) in a two-neck round-bottom flask attached to a Schlenk filter at −78°C. The mixture was warmed up under nitrogen to room temperature over a period of 7 h. The slurry was then filtered under nitrogen, and the white solid was washed with toluene ($3 \times 5$ ml) and then dried under vacuum at room temperature. The yield was 0.815 g. Analytical data appear in Table 2.

### 8.5. Preparation of PQ-*1*-Zr

Twenty milliliters of toluene was added slowly with vigorous stirring to a mixture of 0.800 g PQ-**1** and 0.280 g $Cp_2ZrMe_2$ in a two-neck round-bottom flask attached to a Schlenk filter at −78°C under nitrogen. After 1 h at 25°C, the off-white solid was filtered and washed with hexane and dried under vacuum at room temperature. The weight was 0.805 g. For analytical data, see Table 3.

*8.6. Preparation of PQ-**2**-Zr and PQ-**3**-Zr*

The same procedure as reported for PQ-**1**-Zr was followed with the following reagents: 0.640 g PQ-**2** and 0.231 g $Cp_2ZrMe_2$, resulting in 0.590 g of PQ-**2**-Zr as a yellow solid; 0.891 g PQ-**3** and 0.293 g $Cp_2ZrMe_2$, providing 0.864 g of yellow solid. For analytical data, see Table 3.

*8.7. Preparation of KG-**3**-Zr*

The same procedure as reported for PQ-**1**-Zr was followed with the following reagents: 0.512 g of KG-3 and 0.175 g $Cp_2ZrMe_2$. The isolated product was a pale yellow solid (0.480 g). Analytical data appears in Table 3.

*8.8. Preparation of PQ-Zr and KG-Zr*

A solution of $Cp_2ZrMe_2$ in toluene (0.252 g, 1.00 mmol, 15 ml) was added to 0.500 g of PDS in a round-bottom flask attached to a Schlenk filter and stirred under nitrogen at room temperature in the dark for 3 h. The slurry was filtered under nitrogen, and the solid was washed with dry toluene ($3 \times 5$ ml) and hexane (5 ml). The solid was dried under vacuum (0.601 g). The same procedure was followed for preparation of KG-Zr with the amount of alumina and $Cp_2ZrMe_2$ being 0.309 g and 0.350 g, respectively. The weight of the final product was 0.374 g.

*8.9. Preparation of PQ-MAO-Zr and KG-MAO-Zr*

Adsorption of MAO on PDS and FHA, and impregnation of $Cp_2ZrCl_2$ on these MAO-modified supports involved a literature procedure [16]. The amount of grafted MAO and supported metallocene complex was determined as described previously [16,39].

*8.10. Reaction of $ClB(C_6F_5)_2$ with water*

To a solution containing 0.02 mmol (7.6 mg) $ClB(C_6F_5)_2$ in 0.5 ml of toluene-$d_8$, 0.02 mmol of water was added via syringe. The resulting solution had its $^{19}F$ NMR spectra recorded at room temperature, showing clean formation of $HOB(C_6F_5)_2$ (**4b**). $^{19}F$ NMR (toluene-$d_8$, 25°C) $\delta$ −132.6 (dd, 2F), −149.0 (t, F), −160.9 (m, 2F) ppm. The anhydride, $O[B(C_6F_5)_2]_2$, was formed at room temperature by adding more $ClB(C_6F_5)_2$ or by separate reaction of isolated borinic acid with **3**. $^{19}F$ NMR (toluene-$d_8$, 25°C) $\delta$ −132.8 (dd, 2F), −144.3 (t, F), −160.2 (m, 2F). $^{11}B$ NMR (toluene-$d_8$, 25°C) $\delta$ 40.1. MS (EI): $m/e$ 706 ($M^+$). Anal. calcd. for $C_{24}B_2F_{20}O$: C 40.79, F 53.82. Found: C 40.69, F 53.47.

The reaction of $HB(C_6F_5)_2$ with one equiv. of water under the same conditions also provides the borinic acid.

*8.11. Reaction of $B(C_6F_5)_3$ with water*

To a solution containing 0.02 mmol (10 mg) $B(C_6F_5)_3$ in 0.5 ml of toluene-$d_8$, 0.02 mmol of water was added via syringe. The resulting solution had its $^{19}F$ NMR spectra recorded at room temperature showing clean formation of $H_2O \cdot B(C_6F_5)_3$ (**4b**): $^{19}F$ NMR ($C_7D_8$, 25°C) $\delta$ −134.8 (dd, 2F), −153.6 (t, F), −162.3 (m, 2F) ppm. [10] On heating the solution at 100°C, slow formation of

[10] We note that commercial samples of $B(C_6F_5)_3$ sometimes contain trace amounts of water that leads to line-broadening of the resonance due to the *p*-F atom. The water may be removed by treatment with excess $BCl_3$ in toluene, followed by filtration (to remove boric acid) and recrystallization from hexane–toluene mixtures.

$HOB(C_6F_5)_2$ and $C_6F_5H$ [$^{19}$F NMR $\delta$ −139.2 (m, 2F), −154.3 (t, F), −162.5 (m, 2F)] was observed.

### *8.12. Reaction of $MeB(C_6F_5)_2$ with $Cp_2ZrMe_2$*

A cationic species was formed immediately on mixing $MeB(C_6F_5)_2$ (0.1 mmol) with $Cp_2ZrMe_2$ (0.1 mmol) in benzene-$d_6$ at room temperature [$^1$H NMR (benzene-$d_6$, 25°C) $\delta$ 5.38 (s, Cp, 10H) 0.37 (exchange broadened s, 9H)]. After 60 min at room temperature, this species completely decomposed into $Me_2B(C_6F_5)$ and $Cp_2ZrMe(C_6F_5)$. $Me_2B(C_6F_5)$: $^1$H NMR (benzene-$d_6$, 25°C) $\delta$ 0.97 (t, $J = 2$ Hz, 6H). $Cp_2ZrMe(C_6F_5)$: $\delta$ 5.67 (s, Cp, 10H) and 0.31 (t, $J = 4$ Hz, 3H).

### *8.13. $^{19}$F NMR spectroscopic monitoring of the reaction between boranes **1**–**3** and the supports*

These monitoring experiments were conducted in a Teflon valve-sealed NMR tube with a mole ratio of boron/OH content of the support = 1:1 in toluene-$d_8$ solution at 25°C. $^{19}$F NMR spectra were referenced to tetrafluoro-*p*-xylene, added as an internal standard in known amounts, to quantify the reaction. This data is summarized in Table 2.

### *8.14. $^1$H NMR spectroscopic monitoring of the reaction between $Cp_2ZrMe_2$ and various supports*

These experiments were conducted in a Teflon valve-sealed NMR tube with addition of excess $Cp_2ZrMe_2$, based on the amount of OH content of the support and the modified supports, in benzene-$d_6$ solution at 25°C. $^1$H NMR spectra were referenced to undeuterated benzene, added as an internal standard in known amounts, to quantitate the extent of reaction. The results are summarized in Table 3.

### *8.15. Preparation of $MeB(Ar_F)_2$* [11]

$MeB(C_6F_5)_2$ was synthesized from reaction of **3** and $Cp_2ZrMe_2$ at room temperature in toluene, following removal of the by-product $Cp_2ZrCl_2$. The final pure product was obtained by sublimation at 50–60°C under vacuum ($10^{-3}$ mm Hg). $^1$H NMR ($C_6D_6$, 25°C) $\delta$ 1.39 (quintet, $J_{HF} = 2$ Hz, 3H). $^{19}$F NMR ($C_6D_6$, 25°C) $\delta$ −128.6 (m, 2F), −145.5 (tt, F), −159.9 (m, 2F).

### *8.16. Polymerization procedures and polymer characterization*

#### *8.16.1. Ethylene polymerization*

Toluene solvent (Ominisol grade, VWR/Canlab) used in all polymerizations was freshly purified using a solvent purification system similar to that described in the literature [36] and was delivered to the reactor under pressure from a calibrated sight-glass. Nitrogen and ethylene (Praxair, C.P. grade) was purified by passed through a mixed bed column containing activated BASF R3-11 catalyst/4 Å

[11] We thank Prof. Warren Piers for providing details for this preparation. See also Ref. [40].

molecular sieve, 1:2 w/w). Methylaluminoxane (MAO, 9.6 wt.% Al in toluene; PMAO/*Tol-781) was obtained from Akzo Nobel and concentrated in vacuo to dryness ($10^{-3}$ mm Hg) to provide solid MAO for subsequent use. Triisobutylaluminum (TIBAL) from Aldrich was used as received.

Polymerizations were conducted in a 1-l autoclave equipped with an overhead D.C. motor stirring assembly and a bottom drain valve. The stirring rate was maintained at 500 rpm for all the polymerizations and was initially calibrated with a strobe light. The polymerization temperature was controlled using a Neslab RTE-100 constant temperature bath by circulation of coolant (ethylene glycol/deionized water, 1:1 v/v) through the external, spiral jacket welded to the reactor body. The temperature was monitored/controlled by using a Neslab RTD-220 temperature controller with a Pt RTD sensor immersed in a thermowell inside the reactor. The monomer flow rate was measured with a calibrated Matheson mass flow transducer (Model 8172-0413) connected to a Matheson Multiple Flow Controller (Model 8274). The polymerization profiles (monomer flow rate and solution temperature) were recorded by an IBM PC with a PCL-711s data acquisition card. The progress of the polymerization was monitored in real time using Labtech Acquire data acquisition software, which converted the digital input readings to the desired values using appropriate conversion factors.

In a typical polymerization experiment, the reactor was first conditioned under dynamic vacuum and high temperature (bath temperature around 100°C) for ca. 2 h, during which time the reactor was purged with high purity nitrogen three times. The reactor was then charged with 500 ml of toluene. A desired amount of TIBAL in toluene was added to the stirred reactor via a $N_2$-pressurized stainless steel cylinder (50 ml) prior to heating to the desired temperature. At this point the reactor was saturated with ethylene at 75 psig. The required weight of the supported catalyst was slurred in toluene and was then added to the reactor via the same pressurized cylinder to initiate the polymerization. After a specific period of time, the ethylene flow was stopped and the reactor was vented. The polymer was filtered off, washed with methanol, and then dried in vacuo to constant weight.

*8.16.2. Polymer characterization*

Polymer molecular weights and distributions were determined by gel permeation chromatography (GPC) using a Water 150C chromatograph equipped with a Jordi mixed-bed column ($10–10^3$ Å) employing a differential refractive index detector at 145°C in 1,2,4-TCB solution. Sample dissolution (0.1% w/v) was accomplished by rotating the samples in an oven operating at 160°C for a few h with 0.1% BHT as antioxidant. Samples were eluted at a flow rate of 1.0 ml/min, and columns were calibrated using both a broad MWD PE and narrow MWD PS standards.

DSC analysis was conducted on a Perkin–Elmer DSC-2 Model calibrated using indium metal. A scanning rate of 10°C/min from 25–180°C was employed, and the sample was then cooled to 50°C at 10°C/min to remove all prior thermal history. The second trace was recorded using the same heating program.

The morphologies of the catalyst surface and the nascent polymer particle were examined on a Olympus SZH Optical Microscope and a JEOL JSM-840 scanning electron microscope (SEM), equipped with an energy-dispersed X-ray microanalyzer (EDX), to detect the element distribution on the catalyst surface. SEM was obtained at 2 kV and varying levels of magnification, and the specimens were coated with a 400 Å gold layer by using an electron impact evaporator to increase the conductivity.

The bulk density of polyethylene was determined from the dry weight and the volume of the sample in a volumetric tube by liquid displacement [35].

## Acknowledgements

The authors would like to thank the Natural Sciences and Engineering Research Council of Canada and Nova Chemicals of Calgary, for financial support of this work. The technical assistance of Novachem Research and Technology with some of the SEC analyses is gratefully acknowledged. Finally, we thank Prof. Warren Piers of the University of Calgary for sharing some spectroscopic data for compounds independently prepared and characterized there.

## References

[1] H.H. Brintzinger, D. Fisher, R. Mülhaupt, B. Rieger, R.M. Waymouth, Angew. Chem., Int. Ed. Engl. 34 (1995) 143.
[2] W. Kaminsky, Macromol. Chem. Phys. 197 (1996) 3907.
[3] K. Soga, Macromol. Symp. 101 (1996) 281.
[4] H.C. Welborn, Jr., US Patent 4,701,432, Exxon Chemical Patents, 1987.
[5] H.C. Welborn, Jr., US Patent 4,808,561, Exxon Chemical Patents, 1989.
[6] H.C. Welborn, Jr., US Patent 5,077,255, Exxon Chemical Patents, 1991.
[7] H.C. Welborn, Jr., US Patent 5,183,867, Exxon Chemical Patents, 1993.
[8] M. Kioka, M. Kashiwa, Eur. Pat. 0-285-443, Mitsui Petrochemical Industries, 1988.
[9] T. Takahashi, Eur. Pat. 0-313-386, Mitsubishi Petrochemical Industries, 1988.
[10] J.C.W. Chien, D.W. He, J. Polym. Sci., Part A: Polym. Chem. 215 (1991) 47.
[11] M. Kaminaka, K. Soga, Makromol. Chem., Rapid Commun. 12 (1991) 367.
[12] K. Soga, M. Kaminaka, Makromol. Chem., Rapid Commun. 13 (1992) 221.
[13] K. Soga, M. Kaminaka, Makromol. Chem., Rapid Commun. 15 (1994) 593.
[14] C. Janiak, C.B. Rieger, Angew. Makromol. Chem. 215 (1994) 47.
[15] P. Roos, G.B. Miere, J.J.C. Samson, G. Weichert, K.R. Westerterp, Macromol. Rapid Commun. 18 (1997) 319.
[16] D. Harrison, I.M. Coulter, S. Wang, S. Nistala, B.A. Kuntz, M. Pigeon, J. Tian, S. Collins, J. Mol. Catal., Chem. 128 (1998) 65.
[17] G.G. Hlatky, D.J. Upton, Macromolecules 29 (1996) 8019.
[18] G.G. Hlatky, D.J. Upton, H.W. Turner, WO Patent 91/09882, Exxon Chemical Patents, 1991, and Eur. Pat. 507876B1, 1995.
[19] H.W. Turner, US Patent 5,427,991, Exxon Chemical Patents, 1995.
[20] J.F. Walzer, Jr. WO Patent 96/04319, Exxon Chemical Patents, 1996.
[21] D.G. Ward, E.M. Carnahan, WO Patent 96/23005, W.R. Grace and Co.-CONN., 1996.
[22] A.R. Siedle, R.A. Newmark, W.M. Lamanna, J.C. Huffman, Organometallics 12 (1993) 1491.
[23] A.R. Siedle, W.M. Lamanna, US Patent 5,296,433, Minnesota Mining & Manufacturing Co., 1994.
[24] D.J. Parks, R.E. von, H. Spence, W.E. Piers, Angew. Chem., Int. Ed. Engl. 24 (1995) 809.
[25] R.D. Chambers, T.J. Chivers, J. Chem. Soc. (1965) 3933.
[26] F.J. Feher, T.A. Budzichowski, Polyhedron 14 (1995) 3239.
[27] T.A. Budzichowski, S.T. Chacon, M. Chisholm, F.J. Feher, W.J. Streib, J. Am. Chem. Soc. 113 (1991) 689.
[28] F.J. Feher, K.J. Weller, Inorg. Chem. 30 (1991) 882.
[29] F.J. Feher, D.A. Newman, J. Am. Chem. Soc. 111 (1998) 1741.
[30] W.A. Herrmann, R. Anwander, V. Dufaud, W. Scherer, Angew. Chem., Int. Ed. Engl. 33 (1994) 1285.
[31] T.J. Marks, Acc. Chem. Res. 25 (1992) 57.
[32] K.-H. Dahmen, D. Hedden, R.L. BurWell Jr., T.J. Marks, Langmuir 4 (1988) 1212.
[33] X. Yang, C.L. Stern, T.J. Marks, J. Am. Chem. Soc. 116 (1994) 10015.
[34] N.V. Semikolenova, V.A. Zakharov, Makromol. Chem. Phys. 198 (1997) 2889, and references therein.
[35] G.E. Manger, Porosity and Bulk Density of Sedimentary Rocks, United States Government Printing Office, Washington.
[36] A.B. Pangborn, M.A. Giardello, R.H. Grubbs, R.K. Rosen, F.J. Timmers, Organometallics 15 (1996) 1518.
[37] E. Juaristi, A. Martinez-Richa, A. Garciá-Rivera, J.S. Cruz-Sânchez, J. Org. Chem. 48 (1983) 2603.
[38] E. Samuel, M.D. Rausch, J. Am. Chem. Soc. 95 (1973) 6263.
[39] S. Collins, W.M. Kelly, D.A. Holden, Macromolecules 25 (1992) 1780.
[40] P. Biagini, G. Lugli, F. Garbassi, P. Andreussi, Eur. Pat. Appl. EP 667,357, 1995.